
Hierarchically Disentangled Recurrent Network for Factorizing System Dynamics of Multi-scale Systems

Rahul Ghosh¹ Zachary McEachran² Arvind Renganathan¹ Somya Sharma¹
 Kelly Lindsay¹ Michael Steinbach¹ John Nieber³ Christopher Duffy⁴ Vipin Kumar¹

¹University of Minnesota, Department of Computer Science and Engineering

²NOAA, NWS North Central River Forecast Center

³University of Minnesota, Department of Bioproducts and Biosystems Engineering

⁴Penn State, Department of Civil and Environmental Engineering

{ghosh128, renga016, sharma636, lind0436, stei0062, nieber, kumar001}@umn.edu
 zachary.mceachran@noaa.gov, cxd111@psu.edu

Abstract

We present a knowledge-guided machine learning (KGML) framework for modeling multi-scale processes, and study its performance in the context of streamflow forecasting in hydrology. Specifically, we propose a novel hierarchical recurrent neural architecture that factorizes the system dynamics at multiple temporal scales and captures their interactions. This framework consists of an inverse and a forward model. The inverse model is used to empirically resolve the system’s temporal modes from data (physical model simulations, observed data, or a combination of them from the past), and these states are then used in the forward model to predict streamflow. In a hydrological system, these modes can represent different processes, evolving at different temporal scales (e.g., slow: groundwater recharge and baseflow vs. fast: surface runoff due to extreme rainfall). A key advantage of our framework is that once trained, it can incorporate new observations into the model’s context (internal state) without expensive optimization approaches (e.g., Ensemble Kalman Filtering) that are traditionally used in physical sciences for data assimilation. Experiments with several river catchments from the National Weather Service (NWS) North Central River Forecast Center region show the efficacy of this ML-based data assimilation framework compared to standard baselines, especially for basins that have a long history of observations. Even for basins that have a shorter observation history, we present two orthogonal strategies of training our FHNN framework: (a) using simulation data from imperfect simulations and (b) using observation data from multiple basins to build a global model. We show that both of these strategies (that can be used individually or together) are highly effective in mitigating the lack of training data. The improvement in forecast accuracy is particularly noteworthy for basins where local models perform poorly because of data sparsity. Although we show our proposed framework’s effectiveness in the context of streamflow modeling in hydrology, multi-scale processes are essential in many engineering and scientific applications, making our framework generalizable to such use cases.

1 Introduction

Physical systems, ranging from natural ecosystems to engineered structures, are fundamental to various scientific disciplines and are characterized by complex interactions between internal states and external drivers. These systems’ behaviors are governed by physical states that encapsulate their internal characteristics and determine their responses to external influences. For instance, in

earth and environmental sciences, a catchment’s streamflow response to meteorological drivers like precipitation and temperature is governed by complex physical processes specific to that basin. These processes involve factors such as soil moisture flow, snow-pack melting, and spatiotemporal variations in rainfall. Figure 1 presents a schematic representation of a Forward model, which is crucial for understanding and predicting the behavior of these physical systems. This model framework is widely applicable across fields like environmental sciences and engineering, enabling researchers to simulate complex systems and forecast their future states or behaviors. Accurately capturing and incorporating these physical states is vital for a broad spectrum of applications, as they fundamentally determine how a system responds to external drivers. The forward model approach provides a structured way to represent these relationships, facilitating improved understanding and prediction of system dynamics in various scientific and engineering contexts.

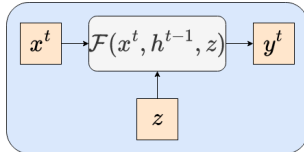


Figure 1: Schematic representation of a Forward model illustrating the functional relationship \mathcal{F} that maps the input x^t along with a latent variable z and the previous hidden state h^{t-1} to the output y^t .

Over the years a number of physics-based models (PBMs) have been developed to model different aspects of the physical systems using mathematical equations. These models have been extensively used for research in understanding the system or in operational settings. For example, for streamflow modeling, the hydrological community makes extensive use of rainfall-runoff models that are built on equations which approximate the underlying bio-geophysical processes of the water cycle, shown in Figure 2(a). These models have been used in operational settings for forecasting streamflow and water levels at NOAA’s National Weather Service (NWS). Such an operational setting requires a forecaster to assimilate real-time observations into the model, i.e. sequential data assimilation [5]. Traditionally this is achieved through variational or Bayesian assimilation methods such as ensemble Kalman Filter (EnKF), that ingests observations in real-time to update the model states (for instance, catchment states in Figure 2(a)). While Process-Based Models (PBMs) are widely adopted in the scientific community, they face challenges in fully capturing the complexity of environmental systems like hydrological catchments. These systems involve aspects such as snow-pack depth, soil moisture distribution, and spatiotemporal variations in rainfall. Many of these relationships between physical characteristics and responses may not be replicated within the structure of a PBM, as they are necessarily approximation of the underlying phenomena. Consequently, this impacts PBMs ability to accurately predict the physical quantities (fluxes) of interest.

In recent years, deep learning techniques have shown tremendous success in a number of computer vision and natural language processing applications. These techniques are becoming increasingly popular in earth science applications including hydrology. Due to the temporal structure in the hydrological cycle, time aware deep learning techniques such as recurrent neural networks (RNNs) have gained prominence as powerful tools for capturing temporal dependencies and building states. Their capacity to process sequential data and model dynamic behaviors makes them well-suited for many physical system applications that require modeling one or more output variables using external inputs. Figure 2(b) illustrates a diagrammatic representation of such ML (RNN) based workflows. In operational settings, two main data assimilation approaches are used for integrating new data into RNN based ML models. The first applies Kalman filter variants to the RNN’s recurrent structure, optimizing a loss function, typically a regularized mean squared error during test time or deployment [22, 18]. The second, more simpler and computationally efficient method employs an auto-regressive RNN, where the previous timestep’s actual output is used as an additional input alongside other weather drivers [7], as shown in Figure 2(c).

Current machine learning models, including RNNs, do not represent states explicitly at multiple temporal scales or model their interactions, limiting their effectiveness for complex physical systems with interdependent multi-scale dynamics. Environmental systems often feature phenomena that evolve at different time scales, from rapid fluctuations to slowly changing trends. For instance, the impact of the location of rainfall on runoff is evident at hourly/daily and seasonal scales. The soil-moisture state of a catchment is built up at weekly scale and thus needs a longer window of

information. On the other hand snow-pack is accumulated at a monthly scale and thus takes longer time to impact runoff of a catchment (snow accumulation in December can impact the stage and discharge in April). Standard RNNs lack the ability to explicitly build states at various temporal scales and model their interactions, which hinders their effectiveness in capturing the full spectrum of system behavior.

In this paper, we propose a novel factorized hierarchical neural network (FHNN) architecture (Figure 2d) that factorizes the system dynamics at multiple temporal scales levels and captures their interactions. This framework consists of an inverse and a forward model. The inverse model is used to empirically resolve the system’s temporal modes from data (physical model simulations, observed data, or a combination of them from the past), and these states are then used in the forward model to predict streamflow. In a hydrological system, these modes can represent different processes, evolving at different temporal scales (e.g., slow: groundwater recharge and baseflow vs. fast: surface runoff due to extreme rainfall). A key advantage of our framework is that once trained, it can incorporate new observations into the model’s context (internal state) without expensive optimization approaches (e.g., Ensemble Kalman Filtering) that are traditionally used in physical sciences for data assimilation.

Experiments with several river catchments from the National Weather Service (NWS) North Central River Forecast Center region show the efficacy of this ML-based data assimilation framework compared to standard baselines, especially for basins that have a long history of observations. Even for basins that have a shorter observation history, we present two orthogonal strategies of training our FHNN framework: (a) using simulation data from imperfect simulations and (b) using observation data from multiple basins to build a global model. We show that both of these strategies (that can be used individually or together) are highly effective in mitigating the lack of training data. The improvement in forecast accuracy is particularly noteworthy for basins where local models perform poorly because of data sparsity. Although we show our proposed framework’s effectiveness in the context of streamflow modeling in hydrology, multi-scale processes are essential in many engineering and scientific applications, making our framework generalizable to such use cases.

2 Problem formulation and Preliminaries

2.1 Problem formulation

This study focuses on learning driver-response behavior for entities. These entities can be physical systems like flux towers, river basins, tasks, people, or domains/distributions. Specifically, we focus on understanding and predicting how precipitation transforms into streamflow at the catchment scale, which is a key part of operational hydrologic forecasting. This problem is referred to as “rainfall-runoff transform”. For a basin, we have access to multiple driver/response pairs of time series sequences, as $\{(\mathbf{x}_1, y_1), (\mathbf{x}_2, y_2), \dots, (\mathbf{x}_T, y_T)\}$, where, $\mathbf{x}_t \in \mathbb{R}^{D_x}$ represents the input vector at time $t \in T$ with D_x dimensions, and $y_t \in \mathbb{R}$ represents the corresponding output. Although in this study y_t is a single scalar target, in many scenarios it can be multiple targets and thus is a simple extension. The goal is to learn a regression function $\mathcal{F} : X \rightarrow Y$ that maps the input drivers to the output response for an entity.

2.2 NWS Model and Operations

The “rainfall-runoff transform”, depends on many meteorological and land-surface characteristics, such as soils, geology, vegetation, snowpack dynamics, and the pattern of rainfall inputs over the land surface. Many of the conceptual and process-based models are developed based on a set of theories (including linearization necessary for the guiding equations to become tractable). At NWS River Forecast Centers (RFCs), a suite of modeling approaches and PBMs are used, ranging from highly detailed first-principles-based models to simple conceptual models of runoff generation mechanisms. The North Central RFC, where model testing and development is ongoing, is responsible for forecasts in the Upper Mississippi River basin through Chester, Illinois, the US side of the Hudson Bay basin, and the western Great Lakes basin. Operational river models of streamflow take catchment-scale precipitation and temperature as inputs, and run on a 6-hourly timescale. Simulated flow is transformed into stream stage, a measure of water surface elevation, according to a stage-discharge rating curve. The North Central RFC then issues stream stage (i.e., elevation) forecasts for many stream gage sites in the US Midwest when the stream water elevation crosses predefined levels

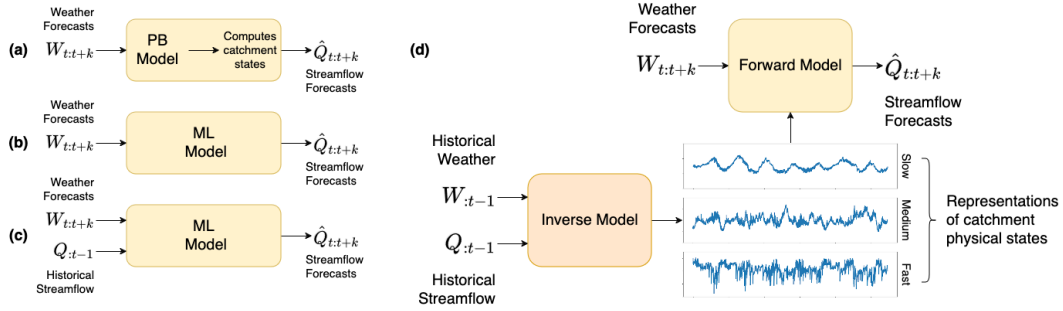


Figure 2: Schematic of different modeling approaches for streamflow forecasting illustrating the inputs, processes, and outputs for each approach. (a) Process-based Models use weather forecasts to estimate catchment states and generate streamflow forecasts. (b) ML-based Forward Models (e.g. LSTM) directly use weather forecasts to predict streamflow forecasts. (c) ML-based Autoregressive Forward Models utilize both weather forecasts and historical streamflow data for streamflow forecasting. (d) Proposed FHNN framework integrates an Inverse Model that generates catchment state representations from historical weather and streamflow data, which are then used alongside weather forecasts in a Forward Model to produce streamflow forecasts, capturing dynamics at multiple temporal scales (slow, medium, fast)

categorized as Minor, Moderate, and Major flooding, which are defined by that elevation’s relative impact to life, property, and the economy at those levels.

Depending on season, snowmelt and rainfall both drive streamflow at different times of year. Thus, precipitation and temperature inputs are first used in a snow model, the NWS Snow-17 model [2]. After rainfall and snowmelt are summed together, this "total water available to the soil profile" is sent into a rainfall-runoff model, which takes in this water and returns the amount of runoff available to the stream. Once the rainfall-runoff model returns the runoff, the timing of when the runoff gets to the streamgauge is accounted for by a Unit Hydrograph. Where tributaries exist, water is routed from upstream to downstream according to "Tatum" attenuation methods.

The centerpiece hydrologic model within the NWS River Forecasting suite of models used at the North Central RFC (and at most RFCs nationwide in the USA) is the Sacramento Soil Moisture Accounting Model (Sac-SMA). Sac-SMA is the model component that transforms rainfall (and/or snowmelt) into runoff. Sac-SMA is a lumped catchment-scale conceptual model with two soil zones, each with reservoirs for soil water tension and free water. Superposition of a primary and secondary lower zone allows for the simulation of more realistic baseflow, and terms in the model allow for interflow, effects of riparian vegetation, variable source area expansion/contraction, and losses to deep groundwater, in addition to Hortonian and saturation excess runoff [6]. Sac-SMA has been shown to have better performance than many rainfall-runoff models in maintaining performance between wet and dry periods [8, 12]. There are 18 major parameters in the Snow-17 and Sac-SMA models combined, in addition to several minor parameters. Calibration is conducted manually by the methods outlined in Anderson et al., 2002[1], wherein the physical meaning of parameters and basin physical characteristics are used to constrain parameter guesses. An iterative approach is taken by an experienced forecaster to vary a parameter while the effect of other parameters is expected to be minimal, assess summary statistics, then proceed. However, this process is time consuming, and inherent interactions within Sac-SMA make it difficult to truly isolate the effect of any one parameter.

A key component of operations at NWS RFCs is daily manual assimilation to align observed and simulated streamflows when they diverge. The PBM used currently are unchanged by observed streamflow: streamflow is their output, deterministically simulated from observed inputs (precipitation and temperature). Divergences between observed and simulated streamflow may be due to input uncertainty, calibration issues, or problems with the inherent physical process representation. To assimilate new streamflow data, a hydrologic forecaster must alter the underlying model states of the PBM manually, such as soil moisture, to incorporate observed streamflow data “on the fly” and to force the model to reproduce observed streamflow behavior. This manual assimilation process is time-consuming, and includes considerable uncertainty as to which among many underlying model states to change in a given operational situation. Alternatively, computationally intensive assimilation routines are necessary, which are often prohibitive for short-fuse operations over large areas. Figure 2(a) shows the diagrammatic representation of the PBM.

2.3 Predictive Modeling for Dynamical Systems

In the realm of machine learning, there exists a class of models dedicated to learning complex transformations from input series $\{x_1, x_2, \dots, x_T\}$ to target variables $\{y_1, y_2, \dots, y_T\}$. Recent strides in deep learning have empowered the automatic extraction of meaningful patterns from multivariate temporal data, significantly enhancing predictions of the target variable. Among temporal deep learning models, RNNs have emerged as a popular choice with successes spanning various applications. To provide some context, a standard RNN is essentially an extended version of a feed-forward neural network, enhanced with feedback connections to facilitate modeling of sequential data. When modeling driver-response relationships, using an RNN equipped with LSTM cells or similar LSTM variants is quite intuitive, as shown in Figure 2 (b). This architecture involves a many-to-many prediction setup, allowing direct mapping of weather inputs to streamflow outputs using a single LSTM network. LSTM, or Long Short-Term Memory, was purposefully developed to combat the common problem of gradient vanishing in RNN training and has evolved into one of the most popular and effective RNN variants. A noteworthy feature of LSTM is its incorporation of an extra memory cell, pivotal for selectively retaining pertinent information from past inputs. In practical terms, it interprets an input sequence and generates a corresponding output sequence iteratively through a set of equations, as shown.

$$\begin{aligned}
 \text{Forget gate : } & f_t = \sigma(W_x^f x_t + W_h^f h_{t-1} + b^f) \\
 \text{Input gate : } & i_t = \sigma(W_x^i x_t + W_h^i h_{t-1} + b^i) \\
 \text{Candidate : } & \tilde{c}_t = \sigma(W_x c_t + W_h h_{t-1} + b) \\
 \text{Context update : } & c_t = f_t \odot \tilde{c}_t + i_t \odot c_{t-1} \\
 \text{Output gate : } & o_t = \sigma(W_x^o x_t + W_h^o h_{t-1} + b^o) \\
 \text{Output : } & h_t = o_t \odot \tanh(c_t)
 \end{aligned} \tag{1}$$

As we wish to conduct regression for continuous values, we generate the predicted response \hat{y}_t at each time step t via a linear combination of hidden units, as:

$$\hat{y}_t = W_y h_t \tag{2}$$

To overcome the challenge of feeding a long time series into a model, the available training data is divided into \mathcal{T} sliding windows of length K during the training phase with/without overlap. The entire framework is trained using a prediction loss, like mean squared error (MSE) as the supervised loss, as shown in equation 3.

$$\mathcal{L} = \frac{1}{\mathcal{T}} \sum_{t=1}^{\mathcal{T}} \sum_{t=1}^K (y_t - \hat{y}_t)^2 \tag{3}$$

2.4 Forecasting for Dynamical Systems

The standard LSTM model cannot ingest near-real time response data and perform data assimilation. Thus a simple extension to the standard LSTM is to provide lagged response data as input to the model. Several studies [7, 17] have shown that auto regression (AR) improves streamflow predictions from LSTMs. A traditional way to train this sequence-to-sequence autoencoder is teacher forcing [20], where ground truth data is used as input instead of the predicted values. Although teacher forcing simplifies the loss landscape and provides faster convergence, this training procedure weakens the encoder as the decoder has to solve a much simpler task. To avoid this the model is trained with a combination of observed and simulated lagged streamflow inputs, a solution known as scheduled sampling [4]. Another class of approaches to solving this problem are professor-forcing methods [14], which uses adversarial learning to encourage a teacher-forcing network (i.e., trained with only observed inputs) to match the fully recursive model. This could be applied to the driver-response modeling if AR models were to exhibit divergent behavior that cannot be solved with scheduled sampling

Even though the LSTM network was proposed to overcome the difficulty in learning long-term dependence, research has shown that LSTM do not have long memory from a statistical perspective [21], due to the presence of the gating mechanisms [3]. In the following section, we will discuss the

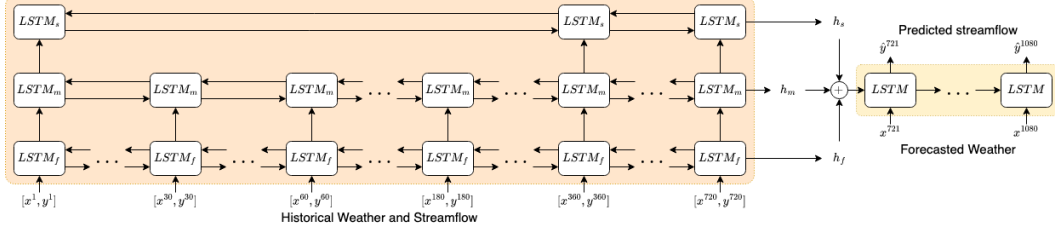


Figure 4: Architecture of FHNN for streamflow prediction. The model processes historical weather and streamflow data at three different timescales (fast, medium, slow) using parallel BiLSTM layers, capturing temporal dependencies at various resolutions. The final hidden states from each timescale (h_f , h_m , h_s) are combined with forecasted weather data to generate streamflow predictions for future time steps. This design allows the model to integrate both short-term fluctuations and long-term trends in the input data for more accurate streamflow forecasting.

LSTM [11] is particularly suited for our task where long-range temporal dependencies between driver and response exist as they are designed to avoid exploding and vanishing gradient problems. The final hidden states for the forward (h_f) and backward LSTM (h_b) are added to get the final embeddings h for each LSTM network, as shown in Figure 4. The internal state (z) of the dynamical system is obtained by first concatenating the slow, medium and fast states and feeding them into an multi-layer perceptron (MLP). Thus the sequence encoder functions are of the form:

$$\begin{aligned}
 [h_t^f]_{1:T}^{\Delta T} &= \text{BiLSTM}([x_t; y_t]_{1:T}^{\Delta T}; \phi_{h_f}) \\
 [h_t^m]_{1:T}^{m\Delta T} &= \text{BiLSTM}([h_t^f]_{1:T}^{m\Delta T}; \phi_{h_m}) \\
 [h_t^s]_{1:T}^{s\Delta T} &= \text{BiLSTM}([h_t^m; h_t^f]_{1:T}^{s\Delta T}; \phi_{h_s}) \\
 z &= \text{MLP}([h_T^s; h_T^m; h_T^f]; \phi_z)
 \end{aligned} \tag{5}$$

where the parameter set ϕ is divided into the LSTM parameters (ϕ_h) and the MLP parameters (ϕ_z). We denote the full encoder using the symbol $\mathcal{E}(y_{1:t}, x_{1:t}; \phi)$. Generally, the encoder can be composed of multi-layers and each layer with several RNNs. In other words, it is a general architecture that varies according to specific tasks.

3.2 Response Decoder

The generator network allows for the conditional generation of response data given the latent variable (z) from the decoder and the driver data. The conditional generative process of the model is given in Figure 3 as follows: for a sequence of historical driver and response data (\mathbf{X}_{hist} and \mathbf{Y}_{hist}), z is obtained from the hierarchical sequence encoder $q_\phi(z|[\mathbf{X}_{hist}; \mathbf{Y}_{hist}])$, and the sequence of response data for the forecast time-period is generated from the decoder $p_\theta(\mathbf{Y}_{forecast}|z, \mathbf{X}_{forecast})$. Specifically we construct an LSTM based conditional sequence generator $y_t = \text{LSTM}(z, x_{T+1:t}; \theta)$, where the encoded internal state of the system (z) is used as the initial state (h^0) of the LSTM model. We denote the decoder based forward model using the symbol $\mathcal{F}(z, x_{T+1:t}; \theta)$.

The model is trained in an end-to-end fashion on the training windows from the training data. The final objective of FHNN during training can be formally expressed as:

$$\arg \min_{\phi, \theta} \frac{1}{K} \sum_{t=T+1}^{T+K} (y^t - \mathcal{F}(z, x_{T+1:t}; \theta))^2 \quad \text{where } z = \mathcal{E}(y_{1:t}, x_{1:t}; \phi) \tag{6}$$

In the inference phase, we receive the current driver and response data for the basin, which we use to create the internal state z . The internal state along with the forecasted driver data is used to make predictions.

3.3 Mitigating lack of Training Data

Environmental systems are highly heterogeneous, i.e., different entities/catchments can have widely different characteristics. Hence, PBMs are often calibrated for each catchment individually. Even in this age of big data, high quality and plentiful observations are available only for a limited number of entities and other entities may have limited data or no data at all. For example, amongst the lakes being studied by United States Geological Survey (USGS), less than 1% of the lakes have 100 or more days of temperature observations and less than 5% of the lakes have 10 or more days of temperature observations [19]. Given their complexity, the RNN-based models trained with limited observed data can lead to poor performance. Thus in this section we present two strategies of training our FHNN framework that mitigates this lack of training data.

3.3.1 Training a single Global Model

ML offers excellent potential for dealing with the high degree of heterogeneity that is always present in environmental systems by leveraging a collection of observations from a diverse set of entities to build a powerful global meta-model. The reason is that ML models can benefit from training data from diverse entities and thus can transfer knowledge across entities. Previously, multi-basin models have shown improved prediction capabilities [15, 13] and have reduced input data needs [9, 10].

Thus, we further develop our integrated KGML framework, called FHNN_{global} to leverage information from multiple basins jointly. Similar to [15] we assign a one-hot vector to each of the basin. The dimension of the one-hot vectors equals the number of catchments. These one-hot vectors originated from the binary vectors used to encode categorical variables in regression, where in our case, the variable is catchment ID. There is one such one-hot binary vector for each basin and these vectors are orthogonal to each other. Regardless of how basins are sorted, one-hot vector assignment assures each basin will be assigned uniquely. The joint optimization objective of FHNN_{global} during training can be formally expressed as:

$$\arg \min_{\phi, \theta} \frac{1}{NK} \sum_{i=1}^N \sum_{t=T+1}^{T+K} (y_i^t - \mathcal{F}(z_i, \mathbf{x}_i^{T+1:t}; \theta))^2 \quad \text{where } z_i = \mathcal{E}(\mathbf{y}_i^{1:t}, \mathbf{x}_i^{1:t}; \phi) \quad (7)$$

3.3.2 Pretraining with Simulation Data

ML models often require an initial choice of model parameters before training. Poor initialization can cause models to anchor in local minimum, which is especially true for deep neural networks. ML models can only learn (however complex) patterns in the data used for training and thus fail on unseen data that is outside the range seen in training. On the other hand, PBMs can make predictions for any arbitrary input variables (e.g., heretofore unseen weather patterns that may result from changing climate). Hence, ML algorithms will need to incorporate scientific knowledge in the ML framework to improve generalization in unseen scenarios. If physical knowledge can be used to help inform the initialization of the weights, model training can be accelerated, requiring fewer epochs for training and needing fewer training samples to achieve good performance.

To address these issues, we propose to pre-train the FHNN model using the simulated data produced by a generic SAC-SMA model, which has been lightly calibrated. In particular, given the input drivers, we run the generic SAC-SMA model to predict the streamflow. These simulated streamflow data are often imperfect but they provide a synthetic realization of physical responses of a basin to a given set of meteorological drivers. Hence, pre-training a neural network using simulations from the SAC-SMA model allows the network to emulate a synthetic but physically realistic phenomena. The model training follows a similar procedure to the standard FHNN training, by just replacing the observed output (y) with the simulated output (y_{sim}), as shown:

$$\arg \min_{\phi, \theta} \frac{1}{K} \sum_{t=T+1}^{T+K} (y_{sim}^t - \mathcal{F}(z, \mathbf{x}_{T+1:t}; \theta))^2 \quad \text{where } z = \mathcal{E}(\mathbf{y}_{sim}^{1:t}, \mathbf{x}_{1:t}; \phi) \quad (8)$$

This process results in a more accurate and physically consistent initialization for the learning model. When applying the pre-trained model to a real system, we fine-tune the model using true observations

as shown in Eq. 6. Here our hypothesis is that the pre-trained model is much closer to the optimal solution and thus requires less observed data to train a good quality model. In our experiments, we show that such pre-trained models can achieve high accuracy given only a few observed data points.

4 Experiments

4.1 Datasets

We evaluate our method to predict streamflow for several river catchments from the National Weather Service (NWS) North Central River Forecast Center (NCRFC) region. Input driver data is limited to catchment-scale Mean Areal Precipitation (MAP) and Mean Areal Temperature (MAT) values at a six-hour time-step, just as needed for the NCRFC operational Sacramento Soil Moisture Accounting Model and Snow-17 suite of models. We select multiple validation basins in the NCRFC area. We split the observed data into “training” and “testing” periods, and assess within the testing period, generally testing between 2012 and 2019. Table 1 shows the training, validation and test time frames for each of the catchment.

Table 1: *Data partitioning for different basins, indicating the periods used for training, validation, and testing.*

Basin ID	Training	Validation	Testing
AGYM5	2001-2009	2010-2011	2012-2019
AMEI4	2001-2009	2010-2011	2012-2019
BCHW3	1987-2009	2010-2011	2012-2019
BEAW3	1986-2009	2010-2011	2012-2019
BIFM5	1997-2009	2010-2011	2012-2019
HWYM5	1994-2009	2010-2011	2012-2019
CVTI2	1995-2009	2010-2011	2012-2019
DARW3	1986-2009	2010-2011	2012-2019
EAGM4	2001-2009	2010-2011	2012-2019
IRNM7	1996-2009	2010-2011	2012-2019
KALI4	1990-2009	2010-2011	2012-2019
MRPM4	1989-2009	2010-2011	2012-2019
RUSI2	1986-2009	2010-2011	2012-2019
STRM4	1989-2009	2010-2011	2012-2019

4.2 Model Setup and Baselines

We compare model performance to multiple baselines, as described below:

- **NWS:** The National Weather Service (NWS) model is a physics-based model that simulates the rainfall-runoff process for catchments. NWS is a one-dimensional, distributed-parameter modeling system that translates spatially-explicit meteorological information into water information, including evaporation, transpiration, runoff, infiltration, groundwater flow, and streamflow.
- **LSTM:** We also assessed model performance of the KGML approach versus other state-of-the-art “out of the box” AI approaches becoming common in hydrology, but that are “black box” models without the added step of estimated hierarchical time-varying catchment states. These AI alternatives include a standard Long Short Term Memory (LSTM) Machine Learning model that takes in precipitation and temperature and generates a streamflow forecast.
- **LSTM-AR:** We train an autoregressive LSTM Machine Learning model that takes in precipitation, temperature, and the most recent observed streamflow as inputs and directly generates a streamflow forecast. This autoregressive ML approach does not generate the catchment representations via an inverse model, but is using the exact same input information as our KGML approach. The structures of the different models attempted are shown in Figure 2.

Note that the NWS and the LSTM model are comparable as both have the exact same amount of information. Similarly, LSTM-AR and FHNN are comparable as both have the previous output available in the data assimilation setting.

4.3 Hyperparameters and Architectures

We create sliding windows of 748 time-steps for the streamflow dataset, strided by the forecast length (28 steps). Here, LSTM takes 720-length sequences (6 months of data) as input and generates output at a stride of 28 steps (7 days). We create input sequences of length 365 using a stride of half the sequence length, i.e., 183. All LSTMs used in the response predictor for FHNN (decoder) and the

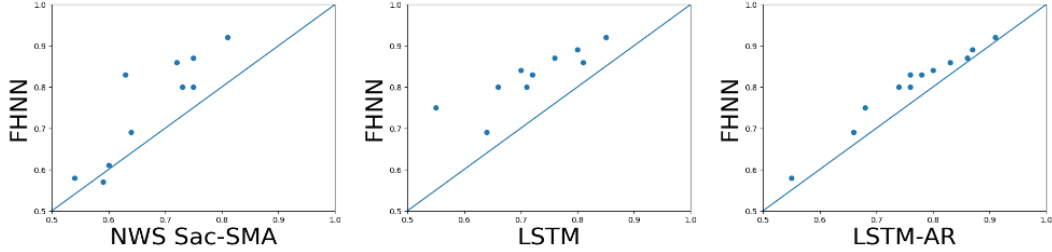


Figure 5: Scatter plot comparison of Nash-Sutcliffe Efficiency (NSE) scores between FHNN and other hydrologic models (NWS Sac-SMA, LSTM, LSTM-AR) across 14 river catchments. Each point represents a catchment, with the diagonal line indicating equal performance.

baselines have one hidden layer with 32 units, whereas the LSTMs used in the encoder of FHNN have a hidden layer with 11 units. The feed-forward network used to get the latent state also has one hidden layer with 32 units. In our experiments, we perform extensive hyperparameter search with the list provided in the Supplementary Material. To reduce the randomness typically expected with network initialization, we report the result of ensemble prediction obtained by averaging predictions from five models with different weight initializations for all architectures (ours and baselines).

We used the Nash-Sutcliffe Model Efficiency (NSE), a widely used metric to measure the predictive skill of hydrologic models. Equation 9 shows the NSE equals one minus the ratio of error variance (MSE) and variance of the observations. When the error variance is larger than the variance of the observations, NSE becomes negative. As a result, NSE ranges from $(-\infty, 1]$, with 1 being a perfect forecast and a negative number being poorer performance in prediction than simply offering the mean historical observation as the forecast. As a measurement metric, the higher NSE means better prediction skills for the investigated models. The NSE was calculated as an average of the NSE for all 7-day forecasts generated by the KGML model, compared to the overall NSE for the NWS model.

$$\text{NSE}(Y, \hat{Y}) = 1 - \frac{\sum_{i=1}^N (\hat{Y}_i - Y_i)^2}{\sum_{i=1}^N (Y_i - \bar{Y})^2} \quad (9)$$

5 Results

5.1 Overall Predictive Performance

Table 2: Model Performance Comparison (Nash-Sutcliffe Efficiency, NSE) of Hydrologic Models Across Multiple Stations

MODELS	AGYM5	AMEI4	BCHW3	BEAW3	BIFM5	HWYM5	CVT12	DARW3	EAGM4	IRNM7	KALI4	MRPM4	RUS12	STRM4
NWS Sac-SMA	0.60	0.73	0.54	0.20	0.16	0.13	0.81	0.59	0.24	0.64	0.75	0.63	0.75	0.72
LSTM	0.14	0.66	0.44	0.55	0.70	0.44	0.85	0.40	0.80	0.64	0.71	0.72	0.76	0.81
LSTM-AR	0.48	0.74	0.55	0.68	0.80	0.76	0.91	0.49	0.87	0.66	0.76	0.78	0.86	0.83
FHNN	0.61	0.80	0.58	0.75	0.84	0.83	0.92	0.57	0.89	0.69	0.80	0.83	0.87	0.86

First, we aim to evaluate how creating states at different levels helps improve the forecast accuracy. We assess the performance of each model based on their forecast accuracy across several NOAA sites. The first row shows the benchmark process-based model SAC-SMA used at NWS with an average NSE of 0.53 across the basins. Standard ML models LSTM and LSTM-AR generally outperform the PBM. By making more effective use of observations, ML models have the potential to address the limitations of traditional PB models that are necessarily approximations of the underlying physical reality. Specifically, the LSTM model improved over the NWS SAC-SMA model by $\sim 15\%$ on mean NSE across test periods in 14 basins. FHNN consistently outperforms other models (by $\sim 6\%$ and $\sim 45\%$ over LSTM-AR and NWS SAC-SMA, respectively, on mean NSE), achieving the highest NSE scores across most stations. This suggests that the FHNN model is highly effective for hydrologic

modeling. Moreover, we observe that for the basins that have low forecast NSE for LSTM-AR, the increase in NSE is more from FHNN.

5.2 Pretraining with Simulation Data

Table 3: Performance comparison (mean and median NSE) of the model on increasing amount of training observation and the availability of simulated data for pretraining. The models are evaluated based on varying amount of training observations, ranging from 0.5 years to 10 years, highlighting the improvement in performance metrics with increased observation durations and the inclusion of simulations. Note that the simulations are obtained from NWS Sac-SMA model with mean and median NSE of 0.53 and 0.61 respectively.

MODELS	Sim: No		Sim: Yes	
	mean	Median	mean	Median
Obs: 0.5 yr	0.18	0.30	0.68	0.75
Obs: 1 yr	0.52	0.53	0.74	0.77
Obs: 2 yr	0.65	0.68	0.77	0.81
Obs: 10 yr	0.77	0.82	0.78	0.82

Here we show the power of pre-training to improve prediction accuracy of the model even with small amounts of training data. A basic premise of pre-training our models is that NWS SAC-SMA simulations, though imperfect, provide a synthetic realization of physical responses of a catchment to a given set of meteorological drivers. Hence, pre-training a neural network using SAC-SMA simulations allows the network to emulate a synthetic realization of physical phenomena. Our hypothesis is that such a pre-trained model requires fewer labeled samples to achieve good generalization performance, even if the SAC-SMA simulations do not match the observations. To test this hypothesis, we pre-train FHNN on the simulated data by minimizing the loss function defined in Equation 8. We further fine-tune the pre-trained FHNN models with two years of observed data and report the performance in Table 3. This model is denoted using the notation “**Sim: Yes Obs: 2yr**” in Table 3. For comparison, we also report the performance of FHNN models that have been trained from scratch using only 2 years of observed data, denoted by “**Sim: No Obs: 2yr**”. Finally we report the FHNN model that has been trained using all the available data denoted by “**Sim: No Obs: All**”. Table 3 shows that pre-training can significantly improve the performance. The improvement is relatively much larger given a small amount of observed data. Even with two years of observed data, a pretrained FHNN achieves NSE similar to that obtained by the model when using all of observed data.

Thus, FHNN has shown that it can learn from a physically-based model and only a small amount of observed data, thereby acting as a model assimilator. These insights from process-based modeling can be used in regions with limited streamflow data. The service ramifications of this result are clear – often, communities have particular stream reaches of concern that cause localized flooding, and desire RFC and NWS services to produce forecasts. However, funding is also often limited, and these communities perhaps fund a streamgage for a year or two hoping it will be enough for NWS to begin forecast services. Calibrated process-based models, however, often need at least 5 years of data to ensure robust calibration for NWS RFC forecast services. The ability of the KGML to learn from a minimal amount of data with the help of model globalization and the use of imperfect process-based models means that potentially years will be taken off the time required to develop robust RFC forecast services. Although additional verification of model robustness in different conditions is underway, initial results show that this is a vision for the not-too-distant future.

5.3 Learning Global Model

Table 4 provides a comprehensive comparison of several models and their global counterparts based on their performance using the Nash–Sutcliffe model efficiency coefficient (NSE) as the evaluation metric. For this study we used a subset of 11 basins out of the available basins. The selected basins are AGYM5, AMEI4, BEAW3, BIFM5, HWYM5, CVTI2, EAGM4, IRNM7, KALI4, MRPM4, and, RUSI2. The models are evaluated using various statistics, including the mean, minimum, 25th percentile, median, 75th percentile, and maximum NSE values. The table provides several key observations. $FHNN_{global}$ exhibits the highest mean NSE value of 0.83 among all the models, indicating that it, on average, performs the best in accurately predicting the target variable. LSTM-AR and FHNN have higher minimum NSE values, indicating better worst-case performance. $FHNN_{global}$

Table 4: Comparison of all the models to their global counterparts using Nash–Sutcliffe model efficiency coefficient (NSE)

Metric	LSTM-AR	FHNN	LSTM-AR _{global}	FHNN _{global}
Mean	0.75	0.80	0.79	0.83
Min	0.48	0.61	0.68	0.71
25%	0.71	0.77	0.74	0.79
Median	0.76	0.83	0.78	0.84
75%	0.83	0.85	0.84	0.87
Max	0.91	0.92	0.92	0.92

again performs the best at the 25th percentile, with a value of 0.79. It is followed closely by LSTM-AR_{global} with 0.74. FHNN_{global} has the highest median NSE value of 0.84, indicating its strong overall performance in predicting the target variable. LSTM-AR_{global} also outperforms its standard version. FHNN_{global} continues to lead in performance at the 75th percentile with a value of 0.87. LSTM-AR_{global} also perform well in this regard. FHNN_{global} achieves the highest maximum NSE value of 0.92, indicating that it can perform exceptionally well in specific cases. LSTM-AR_{global} also reach high maximum NSE values. Thus, the table clearly illustrates that the global configurations of these models generally lead to improved NSE performance compared to their standard counterparts.

6 Discussion

In this section, we delve into a comprehensive discussion of the model in the light of the results presented earlier. Specifically, we will discuss the model on two key aspects: 1) Inferred states of FHNN, and 2) Operationalizing FHNN.

6.1 Visualizing States

The State Encoder (\mathcal{E}) forms a key component of our proposed FHNN as it allows for a deeper understanding and interpretation of the complex dynamics governing physical systems. The inferred states encapsulate the system’s inherent characteristics and behaviors, dictating how the system responds to external influences. FHNN builds states at different temporal scales, capturing both short-term fluctuations and long-term trends. This multi-scale state construction enhances our ability to model and predict the behavior of diverse physical systems, providing a comprehensive understanding and unlocking new insights into their complex dynamics. Thus, it is necessary to evaluate the quality of these inferred states.

In Figure 6, we visualize the slow, medium and fast states from the model for AMEI4, BCHW3, DARW3, EAGM4, KAL4, MRPM4, and STRM4 basins. Recall that each LSTM (slow, medium and fast) in the state encoder has a hidden state dimension of eleven. In this figure we take the mean of the dimensions for each corresponding state and plot them (y-axis) w.r.t. to time (x-axis). This visualization allows for the comparison of different temporal scales of variation within and between the variables, from rapid fluctuations to long-term trends. For each basin, we plot the fast, medium and slow states arranged in columns. The first column with “fast” states exhibit the most variability and detail. The middle column with the “medium” states appears to be a smoothed/filtered version with less high-frequency variation. The last column with “slow” states show an even more smoothed version, capturing only the slowest/long-term trends that are not immediately apparent in the raw data.

As shown in our companion paper [16], these FHNN states have the potential to capture underlying systems dynamics. To demonstrate this potential, FHNN was trained in a synthetic setting using the output of SacSMA as its target data, rather than direct observations. The analysis reveals strong correlation between the FHNN’s internal states and the states of the SacSMA and Snow17 physics-based models. This indicates that FHNN can develop an internal representation that effectively emulates the SacSMA model’s processes, despite not being explicitly programmed with this structure. We argue that this interpretability enhances confidence in FHNN’s ability to learn from physics-based models and suggests potential for future hybrid systems where domain experts could interact with FHNN states.

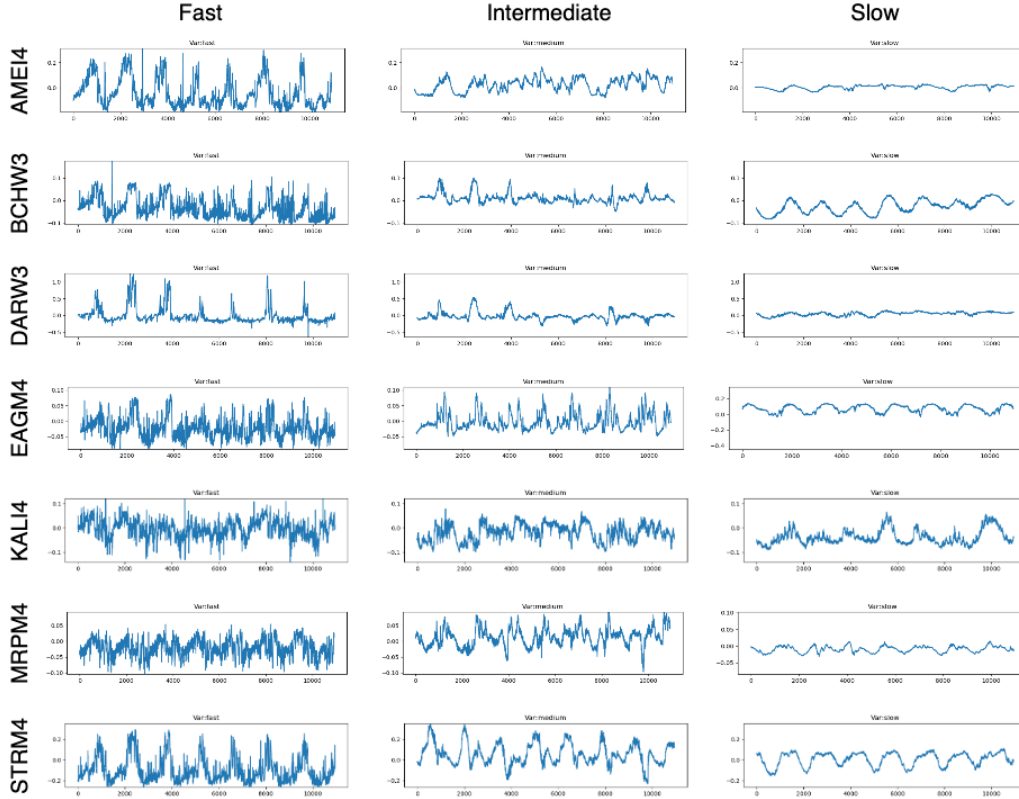


Figure 6: Visualization of FHNN’s inferred fast, medium, and slow states for seven river basins. Each row represents a basin, with columns showing the mean of hidden state dimensions over time for each temporal scale. Fast states (left) exhibit high variability, medium states (center) show smoothed patterns, and slow states (right) capture long-term trends.

6.2 Operational Results

Our companion paper [16] compares the performance of FHNN, with NWS-issued forecasts for flood prediction in the KALI4 basin in Central Iowa. Using archived Quantitative Precipitation Forecasts and perfect temperature forecasts, FHNN outperformed NWS forecasts in 7 out of 12 major flood events tested. The results show that while human forecasters added significant value in the first 12 hours, after which FHNN showed similar performance up to 2 days and superior accuracy beyond that point. This demonstrates FHNN’s potential to improve flood forecasting, particularly for longer-term predictions, by overcoming limitations in the base Sac-SMA model used by NWS.

7 Conclusion

This paper presents a novel approach to modeling dynamical systems using a factorized hierarchical neural network (FHNN). The proposed method demonstrates significant improvements in predictive performance under the data assimilation setting in hydrologic forecasting. By incorporating hierarchical state representations at multiple temporal scales, the FHNN model effectively captures complex dependencies in sequential data, outperforming traditional LSTM-based auto-regressive models. Experimental results of our study demonstrate the effectiveness of the Factorized Hierarchical Neural Network (FHNN) model in improving hydrologic forecasting compared to traditional models like the NWS Sac-SMA and standard LSTM-based auto-regressive approaches for data assimilation.

References

- [1] Eric A Anderson. Calibration of conceptual hydrologic models for use in river forecasting. *Office of Hydrologic Development, US National Weather Service, Silver Spring, MD*, 372, 2002.
- [2] Eric Andrew Anderson. *A point energy and mass balance model of a snow cover*. Stanford University, 1976.
- [3] Francois Belletti, Alex Beutel, Sagar Jain, and Ed Chi. Factorized recurrent neural architectures for longer range dependence. In *international conference on artificial intelligence and statistics*, pages 1522–1530. PMLR, 2018.
- [4] Samy Bengio, Oriol Vinyals, Navdeep Jaitly, and Noam Shazeer. Scheduled sampling for sequence prediction with recurrent neural networks. *Advances in neural information processing systems*, 28, 2015.
- [5] Laurent Bertino, Geir Evensen, and Hans Wackernagel. Sequential data assimilation techniques in oceanography. *International Statistical Review*, 71(2):223–241, 2003.
- [6] Robert JC Burnash. *A generalized streamflow simulation system: Conceptual modeling for digital computers*. US Department of Commerce, National Weather Service, and State of California . . . , 1973.
- [7] Dapeng Feng, Kuai Fang, and Chaopeng Shen. Enhancing streamflow forecast and extracting insights using long-short term memory networks with data integration at continental scales. *Water Resources Research*, 56(9):e2019WR026793, 2020.
- [8] Keirnan JA Fowler, Murray C Peel, Andrew W Western, Lu Zhang, and Tim J Peterson. Simulating runoff under changing climatic conditions: Revisiting an apparent deficiency of conceptual rainfall-runoff models. *Water Resources Research*, 52(3):1820–1846, 2016.
- [9] Rahul Ghosh, Arvind Renganathan, Kshitij Tayal, Xiang Li, Ankush Khandelwal, Xiaowei Jia, Christopher Duffy, John Nieber, and Vipin Kumar. Robust inverse framework using knowledge-guided self-supervised learning: An application to hydrology. In *Proceedings of the 28th ACM SIGKDD Conference on Knowledge Discovery and Data Mining*, pages 465–474, 2022.
- [10] Rahul Ghosh, Haoyu Yang, Ankush Khandelwal, Erhu He, Arvind Renganathan, Somya Sharma, Xiaowei Jia, and Vipin Kumar. Entity aware modelling: A survey. *arXiv preprint arXiv:2302.08406*, 2023.
- [11] Alex Graves and Jürgen Schmidhuber. Framewise phoneme classification with bidirectional lstm and other neural network architectures. *Neural networks*, 18(5-6):602–610, 2005.
- [12] Andrew John, Keirnan Fowler, Rory Nathan, Avril Horne, and Michael Stewardson. Disaggregated monthly hydrological models can outperform daily models in providing daily flow statistics and extrapolate well to a drying climate. *Journal of Hydrology*, 598:126471, 2021.
- [13] Frederik Kratzert, Daniel Klotz, Guy Shalev, Günter Klambauer, Sepp Hochreiter, and Grey Nearing. Towards learning universal, regional, and local hydrological behaviors via machine learning applied to large-sample datasets. *Hydrology and Earth System Sciences*, 23(12):5089–5110, 2019.
- [14] Alex M Lamb, Anirudh Goyal ALIAS PARTH GOYAL, Ying Zhang, Saizheng Zhang, Aaron C Courville, and Yoshua Bengio. Professor forcing: A new algorithm for training recurrent networks. *Advances in neural information processing systems*, 29, 2016.
- [15] Xiang Li, Ankush Khandelwal, Xiaowei Jia, Kelly Cutler, Rahul Ghosh, Arvind Renganathan, Shaoming Xu, Kshitij Tayal, John Nieber, Christopher Duffy, et al. Regionalization in a global hydrologic deep learning model: from physical descriptors to random vectors. *Water Resources Research*, 58(8):e2021WR031794, 2022.
- [16] Zac McEachran, Rahul Ghosh, Arvind Ranganathan, Somya Sharma, Kelly Lindsay, Michael Steinbach, John Nieber, Christopher Duffy, and Vipin Kumar. Knowledge-guided machine learning for data assimilation and interpretable operational flood forecasting. *Water Resources Research*, in submission, 2024.
- [17] Zach Moshe, Asher Metzger, Gal Elidan, Frederik Kratzert, Sella Nevo, and Ran El-Yaniv. Hydronets: Leveraging river structure for hydrologic modeling. *arXiv preprint arXiv:2007.00595*, 2020.

- [18] Grey S Nearing, Daniel Klotz, Alden Keefe Sampson, Frederik Kratzert, Martin Gauch, Jonathan M Frame, Guy Shalev, and Sella Nevo. Data assimilation and autoregression for using near-real-time streamflow observations in long short-term memory networks. *Hydrology and earth system sciences discussions*, 2021:1–25, 2021.
- [19] Emily K Read, Lindsay Carr, Laura De Cicco, Hilary A Dugan, Paul C Hanson, Julia A Hart, James Kreft, Jordan S Read, and Luke A Winslow. Water quality data for national-scale aquatic research: The water quality portal. *Water Resources Research*, 53(2):1735–1745, 2017.
- [20] Ronald J Williams and David Zipser. A learning algorithm for continually running fully recurrent neural networks. *Neural computation*, 1(2):270–280, 1989.
- [21] Jingyu Zhao, Feiqing Huang, Jia Lv, Yanjie Duan, Zhen Qin, Guodong Li, and Guangjian Tian. Do rnn and lstm have long memory? In *International Conference on Machine Learning*, pages 11365–11375. PMLR, 2020.
- [22] Jacob A Zwart, Samantha K Oliver, William David Watkins, Jeffrey M Sadler, Alison P Appling, Hayley R Corson-Dosch, Xiaowei Jia, Vipin Kumar, and Jordan S Read. Near-term forecasts of stream temperature using deep learning and data assimilation in support of management decisions. *JAWRA Journal of the American Water Resources Association*, 59(2):317–337, 2023.